NATIONAL ADVISORY COMMITTEE FOR AERONAUTICS

TECHNICAL NOTE 3539

SOME EFFECTS OF SYSTEM NONLINEARITIES IN THE PROBLEM OF AIRCRAFT FLUTTER

By Donald S. Woolston, Harry L. Runyan, and Thomas A. Byrdsong

Langley Aeronautical Laboratory
Langley Field, Va.

NACA

Washington
October 1955

NATIONAL ADVISORY COMMITTEE FOR AERONAUTICS

TECHNICAL NOTE 3539

SOME EFFECTS OF SYSTEM NONLINEARITIES IN THE PROBLEM OF AIRCRAFT FLUTTER

By Donald S. Woolston, Harry L. Runyan,
and Thomas A. Byrdsong

SUMMARY

This paper presents the results of a preliminary investigation of the effect of nonlinear structural terms on the flutter of a two-degree-of-freedom system. The three types of nonlinearities investigated were a flat spot, hysteresis, and a cubic spring. Calculations were made on an analog computer. For one case, the flat spot, an experimental investigation was also made and good correlation with theory was found.

In general, it was found that the linear flutter speed did not change for small disturbance angles; however, for larger disturbance or input angles, the flutter speed usually decreased. One exception was the cubic hard spring, for which a limited-amplitude flutter was found to exist well above the linear flutter speed.

INTRODUCTION

Until fairly recently the problem of aircraft flutter has been treated analytically as a purely linear phenomenon. Potentially, however, many sources of nonlinearities exist and their possible effects are receiving more and more attention. It is thought, for example, that many of the limited-amplitude oscillations are associated with nonlinearities.

In the flutter problem three types of forces - the inertia, the damping, and the elastic - are involved. Each of these forces may arise from either the aerodynamics of the problem or from the structure. Nonlinearities associated with the aerodynamics may arise, for example. from the effects of thickness or flow separation or from the variation in hinge moments with amplitude. Some aerodynamic effects of thickness have been studied analytically by Van Dyke (ref. 1). He has treated the case of two-dimensional, supersonic flow and has found, except near a Mach number of 1, that thickness effects for this case are moderate.

The structural side of the problem may also give rise to nonlinearities in the inertial, damping, and elastic forces. The present

investigation is concerned with nonlinearities in the elastic forces, and three types of nonlinear springs have been considered. Their effects on flutter have been examined in the investigation of a two-dimensional, two-degree-of-freedom system. A part of the investigation has been made on an electronic analog computer. The analog representation of the problem is discussed in the appendix.

SYMBOLS

ω_h	natural frequency in translation, radians/sec
ω_α	natural frequency in pitch for basic linear system, radians/sec
I_α	mass moment of inertia about elastic axis per unit length of span, slug-ft^2/ft
K_θ	spring constant of linear system, ft-lb/radian
M	moment, ft-lb
m	mass per unit length, slugs/ft
S_α	mass static unbalance per unit length, referred to elastic axis, slug-ft/ft
V	flutter speed
V_{LIN}	flutter speed of linear system
x_{cg}	coordinate of center of gravity measured from leading edge, percent chord
x_{ea}	coordinate of elastic axis measured from leading edge, percent chord
δ_T	angular free play, deg
θ	angle of rotation, deg unless indicated otherwise
ρ	fluid density, slugs/cu ft
a	nondimensional distance of pitch axis from midchord measured in half-chords, positive for positions of pitch axis behind midchord, $a = 2x_{ea} - 1$
b	wing semichord, ft
h	vertical displacement from equilibrium, ft
t	time, sec

Dot over quantity indicates differentiation with respect to time.

TYPES OF NONLINEAR SPRINGS INVESTIGATED

Nonlinearities in the elastic forces can arise in many possible ways. Three types of nonlinear springs have been considered, and their characteristics are shown as plots of the force or moment required to produce a given displacement. (See fig. 1.)

Shown at the left of the figure is a flat spot. This may be considered to represent the condition of free play in the hinge or linkage of a control system.

At the right of the figure is one type of hysteresis. As force or moment is increased, displacement varies in a linear manner until a point is reached at which a jump occurs, after which the system is again linear. On the return path, a corresponding jump occurs at a negative value of the force. A nonlinearity of this type may occur in the case of a control surface with free play if friction exists at some point in the linkage, or it may occur through the action of power servos. In the case of a wing, this type of nonlinearity might represent the effect of rivet slip.

The third type of nonlinearity treated has been termed a cubic spring, where the force exerted depends on the usual linear power of the displacement and, in addition, on a term containing the cube of the displacement. This can be considered either as a hard spring, which becomes stiffer as displacement increases, as shown by the solid line, or as a soft spring, which becomes weaker as displacement increases, as shown by the dashed line. In the case of a control surface, a hard-spring effect might be associated with power controls. In the case of a structure, a hardening effect is found when a thin wing, or perhaps a propeller, is subjected to increasing amplitudes of torsion. A soft-spring effect may be associated with panel buckling.

EFFECTS OF NONLINEAR SPRINGS ON AIRCRAFT FLUTTER

These three types of nonlinearities have been considered in the flutter investigation of a two-dimensional, two-degree-of-freedom system, free to oscillate in translation and in pitch. The flutter characteristics of the system have been determined with an electronic analog computer, using incompressible, indicial air forces. The analog representation of the fundamental linear flutter equations was based on the work of Baird, Pines, and Winson (ref. 2). For the flat spot, in addition to the analog results, experimental results have been obtained

in the Langley 2- by 4-foot flutter research tunnel. The physical characteristics of the systems treated for each of the three types of nonlinear springs are given in table I.

In the flutter results to be discussed, one of the variables to be employed is an input angle θ. The significance of this input angle is given in the following discussion.

In obtaining results with the analog computer for a particular case, a given value of velocity is selected, the system is given an initial displacement (for example, θ), and its response to this displacement is examined for stability. In general, the results to follow will show that the response of the system becomes unstable only when a sufficiently large initial displacement is imposed. In the physical system, this initial displacement corresponds to the effect of a gust or to an abrupt movement of the control stick.

Flutter Results With the Cubic Spring

In figure 2, analog results are shown for the cubic spring in the torsional degree of freedom. Results are shown in the form of the input angle θ required to induce flutter as a function of velocity. For this case, the relation between moment and displacement was arbitrarily assumed to be $M = 140.5\theta + 4000\theta^3$, where M is the moment in foot-pounds and θ the torsional displacement in radians. The coefficient of the linear term in θ represents the spring constant in foot-pounds per radian of the linear system.

First, the flutter speed of the linear system was investigated and was found to be around 270 feet per second. Then, both hard and soft cubic springs were considered. Flutter boundaries are shown by the solid curve for the soft spring and by the dashed line for the hard spring. In both cases, the flutter region lies to the right of the boundary.

For the hard spring, the flutter boundary is a straight line at the flutter speed of the linear system. The soft spring in this case had a destabilizing effect in that flutter could be induced below the linear flutter speed by making the initial displacement sufficiently large. For the system treated herein, however, the deviation from the linear flutter speed occurs only at fairly high initial displacements.

It is also of interest to consider the flutter amplitudes associated with these results. For both the linear system and the soft spring, the flutter oscillation was highly divergent at any velocity above the flutter boundary. With the hard spring in the system, however, the flutter amplitude is self limited. This limit amplitude is a function of velocity, however, and increases as velocity is increased beyond the flutter boundary.

In studying other configurations, cases have been found in which a hard spring can be destabilizing, and it appears that the effects produced by a cubic spring depend on the stiffnesses of the original linear system. Generally, flutter speed decreases as the bending-torsion frequency ratio approaches unity. If a cubic spring, whether hard or soft, tends to make this ratio approach unity, it will probably be destabilizing.

Flutter Results With the Flat Spot

The second type of nonlinearity to be considered is the flat spot and, as mentioned previously, both wind-tunnel and analog studies were made. The main features of the model used in the wind-tunnel tests are shown in figure 3. The sketch represents a two-dimensional model which completely spans the test section and which is free to oscillate in pitch and translation. The pitching degree of freedom is provided by a bearing-supported shaft located slightly behind the quarter chord. This system in turn is suspended between a pair of leaf springs on either side of the test section so that the entire mechanism is free to translate.

In translation the system is linear. The nonlinearity was introduced in the torsional degree of freedom in the manner shown in the detail sketch. A leaf spring is clamped to the end of the torsion axis and its free end extends upward between two set screws. The gap between the screws can be closed completely to give a linear torsion spring or opened to provide any desired amount of angular free play, giving the spring characteristic shown to the right in figure 3.

In figure 4, results obtained in the wind tunnel with this configuration are compared with analog results. The ordinate of the figure is again the input angle θ in degrees. The abscissa is a flutter-speed ratio V/V_{LIN}, where V_{LIN} is the flutter speed of the linear system, and it is immediately seen that the flutter speeds have been decreased. In the investigation the angular free play δ_T was kept constant at 0.5°. The solid curves and the regions labeled stable, mild flutter, and flutter refer to the analog results. The circles show wind-tunnel experimental points.

In both the experiment and the analog results, a preload was incorporated into the system. This preload was comparable in effect to a deflected tab and produced a moment which varied with the velocity. At equilibrium, therefore, the model was not centered in the flat spot but rather at some point on the linear arm of the diagram. This means that, for small displacements from equilibrium, the system moved only on this linear arm so that, at velocities below the linear flutter speed, the system was stable.

With displacements slightly greater than 0.5°, the effect of the flat spot began to enter the picture and a region of mild, limited-amplitude flutter was encountered. Here the system oscillated about its equilibrium position across only one knee of the flat spot and did not traverse the full flat-spot width.

As an example, at a value of the flutter-speed ratio of 0.6, the flutter amplitude in this region of mild flutter was about 1°. Such limited oscillations, when translated into the behavior of control surfaces in flight, might not be dangerous in themselves but could be significant from a fatigue standpoint.

As initial inputs were increased still further, a much more violent flutter was encountered in which the model oscillated completely through the flat spot with large amplitude. The experimental wind-tunnel points apply to this violent type of flutter and agreement with the analog results is fairly good. Although not shown in the figure, it should be noted that in the experimental tests, also, a region of mild flutter was encountered at initial displacements comparable to those indicated by the analog.

In obtaining these results, only a single value of the preload has been taken into account, and further studies in which the preload is varied would be desirable. The destabilizing effect of the flat spot in this case is probably associated with an effective reduction in torsional stiffness. In the absence of any preload, the torsional stiffness at equilibrium would be reduced to zero, and presumably then one would at least expect to encounter unstable oscillations in the region of the flat spot.

Flutter Results With Hysteresis

If, in addition to the free play, some source of static friction exists, the hysteresis phenomenon occurs. As mentioned previously, a hysteresis of the type described may arise in the case of friction in the hinge or linkage of a control surface or, in the case of a wing, might be associated with rivet slip.

Before considering the flutter results with hysteresis, some purely structural characteristics of the system with hysteresis should be examined. Shown in figure 5 is the response of a system with hysteresis at zero airspeed. The upper and lower traces represent, respectively, the displacement of the system and the variation in moment after release from the initial displacement from equilibrium. The indentations on the lower trace occur when the system passes through the flat spots of the hysteresis box.

The presence of this hysteresis in the system has two primary effects on the structural characteristics. One is the introduction of variable structural damping, shown by the lines drawn tangent to the upper trace. At high amplitudes, the rate of decay is relatively small. As the amplitude of the oscillation approaches the height of the hysteresis box, the damping is considerably greater. When the oscillation is contained within the box, the structural damping in this illustration is zero.

The second effect of the hysteresis on the structural properties of the system is not apparent in this figure but is the introduction of an effectively weaker spring. At high amplitudes the frequency of the oscillation is less than the frequency at low amplitudes where the system is linear.

Analog results for bending-torsion flutter with hysteresis in the torsional degree of freedom are shown in figure 6. Results are again presented in the form of the input angle θ plotted against flutter velocity. Two values of δ_T, the amount of free play in torsion or the width of the hysteresis box, were considered. These were δ_T of 0.2°, shown by the solid line, and $\delta_T = 0.4^\circ$, shown by the dashed line. The height of the hysteresis box was held constant. In these results, the flutter region lies above or to the right of the lines.

Consider first the results for δ_T of 0.2°, shown by the solid curve. For very small inputs, the system oscillates on a line through the center of the box with a linear spring constant, as shown by the dashed line in the spring diagram. For this reason, the flutter boundary at the highest velocity occurs at the flutter speed of the linear system.

This boundary continues straight upward until an initial displacement of 0.6° is imposed. Actually an initial displacement greater than 0.2° represents a displacement beyond the linear path within the hysteresis box. At low amplitudes, since the presence of the hysteresis introduces a large amount of structural damping, for inputs up to 0.6° the oscillation decays and the system oscillates at constant amplitude within the hysteresis box. For larger displacements at the linear flutter speed and at velocities above the linear flutter speed, the oscillation diverged rapidly.

As in the case of the flat-spot results, flutter could be induced at velocities below the linear flutter speed by making the initial displacements sufficiently large. At the larger displacements, the

hysteresis damping is smaller and the presence of the free play in the system is producing an effectively weaker spring. Finally a velocity is reached below which the air forces will not sustain an oscillation regardless of the magnitude of the initial displacement. For all velocities below the linear flutter speed, the flutter is of limited amplitude.

Results for the wider hysteresis box exhibit the same trends. At velocities below the linear flutter speed, however, greater initial displacements are required to initiate flutter, since the wider hysteresis box introduces more damping. At the same time, the increased amount of free play reduces the effective spring constant even more, and the region of limited-amplitude flutter extends to a lower velocity.

CONCLUDING REMARKS

Little is known of the exact nature and magnitude of the nonlinearities which exist in actual aircraft. The purpose herein has been to make a preliminary study of the effects of some nonlinearities which might occur. The results shown are, of course, a function of the particular configurations treated and are perhaps most closely related to the problem of control-surface flutter. They indicate, however, that in some cases nonlinear effects can be large and can be destabilizing. The results indicate further that the stability of a nonlinear system can become a function of the magnitude of an external excitation; it is also indicated that, when a nonlinear system becomes unstable, its flutter may become less violent and self-limited.

Langley Aeronautical Laboratory,
National Advisory Committee for Aeronautics,
Langley Field, Va., May 9, 1955.

APPENDIX A

ANALOG REPRESENTATION OF NONLINEAR FLUTTER EQUATIONS

In this appendix the wiring diagrams for the various types of nonlinearities which have been treated are considered. In figure 7, a diagram is given which shows the wiring for the analog representation of the equations of motion for the complete system with the dashed box indicating the point at which the nonlinearities are introduced. Figures 8, 9, and 10 show, respectively, the wiring for the cubic spring, the flat spot, and the hysteresis nonlinearity. The function θ_n shown in figures 9 and 10 denotes the output of the nonlinear circuits.

The form of the basic equations of motion used in the wiring is essentially that given by reference 2. In reference 2 the equations of motion are general in that they are written in terms of coupled modes of vibration and provide for spanwise variations in structural properties and in deflections. In the present analysis a two-dimensional system oscillating in rigid modes of translation h and pitch θ is considered. For this case the equations of motion can be written in the following form:

For the translational degree of freedom,

$$-\ddot{h} = \frac{1}{A_{11}^{2}}\left[A_{11}^{1}\dot{h} + A_{11}^{0}h + A_{12}^{2}\ddot{\theta} + A_{12}^{1}\dot{\theta} + A_{12}^{0}\theta + \right.$$

$$A_{11}^{3}\int_0^{\tau}\phi(\tau-\tau_1)h(\tau-\tau_1)\,d\tau_1 + A_{12}^{3}\int_0^{\tau}\phi(\tau-\tau_1)\theta(\tau-\tau_1)\,d\tau_1 +$$

$$A_{11}^{4}\int_0^{\tau}\phi(\tau-\tau_1)\ddot{h}(\tau-\tau_1)\,d\tau_1 + A_{12}^{4}\int_0^{\tau}\phi(\tau-\tau_1)\ddot{\theta}(\tau-\tau_1)\,d\tau_1 +$$

$$\left.A_{11}^{3}\phi(\tau)h(0) + A_{11}^{4}\phi(\tau)\dot{h}(0) + A_{12}^{3}\phi(\tau)\theta(0) + A_{12}^{4}\phi(\tau)\dot{\theta}(0)\right] \qquad (A1)$$

and for the pitch degree of freedom,

$$-\ddot{\theta} = \frac{1}{A_{22}^2}\left[A_{21}^2\ddot{h} + A_{21}^1\dot{h} + A_{21}^0 h + A_{22}^1\dot{\theta} + A_{22}^0\theta + \right.$$

$$A_{21}^3 \int_0^\tau \phi(\tau-\tau_1)h(\tau-\tau_1)\,d\tau_1 + A_{22}^3 \int_0^\tau \phi(\tau-\tau_1)\theta(\tau-\tau_1)\,d\tau_1 +$$

$$A_{21}^4 \int_0^\tau \phi(\tau-\tau_1)\ddot{h}(\tau-\tau_1)\,d\tau_1 + A_{22}^4 \int_0^\tau \phi(\tau-\tau_1)\ddot{\theta}(\tau-\tau_1)\,d\tau_1 +$$

$$\left. A_{21}^3\phi(\tau)h(0) + A_{21}^4\phi(\tau)\dot{h}(0) + A_{22}^3\phi(\tau)\theta(0) + A_{22}^4\phi(\tau)\dot{\theta}(0)\right] \qquad (A2)$$

where $\tau = Vt/b$ is a nondimensional time factor and τ_1 is the variable of integration. For the cases considered, the quantities appearing in these equations are defined as

$$\left.\begin{aligned}
A_{11}^2 &= m + \pi\rho b^2 & A_{21}^2 &= S_\alpha - \pi\rho b^3 a \\
A_{11}^1 &= 2\pi\rho b^2 & A_{21}^1 &= -2\pi\rho b^3\left(\tfrac{1}{2} + a\right) \\
A_{11}^0 &= \left(\frac{\omega_h b}{V}\right)^2 m & A_{21}^0 &= 0 \\
A_{12}^2 &= S_\alpha - \pi\rho b^3 a & A_{22}^2 &= I_\alpha + \pi\rho b^4\left(\tfrac{1}{8} + a^2\right) \\
A_{12}^1 &= 2\pi\rho b^3(1 - a) & A_{22}^1 &= 2\pi\rho b^4 a\left(a - \tfrac{1}{2}\right) \\
A_{12}^0 &= 2\pi\rho b^3 & A_{22}^0 &= \left(\frac{\omega_\alpha b}{V}\right)^2 I_\alpha - 2\pi\rho b^4\left(a + \tfrac{1}{2}\right) \\
A_{11}^3 &= 0 & A_{21}^3 &= 0 \\
A_{12}^3 &= -2\pi\rho b^3 & A_{22}^3 &= 2\pi\rho b^4\left(a + \tfrac{1}{2}\right) \\
A_{11}^4 &= -2\pi\rho b^2 & A_{21}^4 &= 2\pi\rho b^3\left(a + \tfrac{1}{2}\right) \\
A_{12}^4 &= -2\pi\rho b^3\left(\tfrac{1}{2} - a\right) & A_{22}^4 &= 2\pi\rho b^4\left(\tfrac{1}{4} - a^2\right)
\end{aligned}\right\} \qquad (A3)$$

The term $\phi(\tau)$ is the "lift-deficiency function" obtained from the approximate expression by Robert T. Jones (ref. 3) for Wagner's indicial response function (ref. 4) and appears as

$$\phi(\tau) = a_1 e^{\beta_1 \tau} + a_2 e^{\beta_2 \tau} \tag{A4}$$

where

$$a_1 = 0.165 \qquad a_2 = 0.335$$

$$\beta_1 = -0.0455 \qquad \beta_2 = -0.30$$

The nonlinearities were introduced in the pitch degree of freedom and were represented by circuits which correspond to the spring-characteristic diagrams in figure 1. The nonlinearities are associated with the first term of A_{22}^0. In the case of the cubic spring (fig. 8) the torsional frequency ω_α appearing in A_{22}^0 was expressed in terms of the moment function $M = K_\theta \theta + C\theta^3$ which was assumed for the spring-characteristic diagram of figure 2.

Potentiometer settings for the diagram of the equations of motion in figure 7 are given in table II.

REFERENCES

1. Van Dyke, Milton D.: Supersonic Flow Past Oscillating Airfoils Including Nonlinear Thickness Effects. NACA TN 2982, 1953.

2. Baird, Eugene F., Pines, Samuel, and Winson, Jonathan: The Solution of Two Problems of Four Degree of Freedom Flutter by Electronic Analogue Computation. Project Cyclone (Contract N6 ORI-128, Task Three - NR-725-001), Reeves Instrument Corp. (New York City), Feb. 1952.

3. Jones, Robert T.: Operational Treatment of the Nonuniform-Lift Theory in Airplane Dynamics. NACA TN 667, 1938.

4. Wagner, Herbert: Über die Entstehung des dynamischen Auftriebes von Tragflügeln. Z.a.M.M., Bd. 5, Heft 1, Feb. 1925, pp. 17-35.

TABLE I.- CHARACTERISTICS OF SYSTEMS

Parameter	Systems		
	Cubic	Flat spot	Hysteresis
Semichord, ft	0.5	0.5	0.5
x_{ea}, percent chord	23.0	29.7	23.0
x_{cg}, percent chord	25.6	31.8	25.6
m, slugs/ft	0.1489	0.2985	0.1489
S_α, slug-ft/ft	0.003871	0.00321	0.003871
I_α, slug-ft^2/ft	0.008934	0.01196	0.008934
ω_h, radians/sec	94.25	58.94	66.60
ω_α, radians/sec	125.66	81.24	125.66
ρ, slugs/cu ft	0.002378	0.00243	0.002378

TABLE II.- POTENTIOMETER SETTINGS

[S.F. = Scale factor = 2,000 volts/unit]

Potentiometer number	Setting	Potentiometer number	Setting
①	0.1	⑰	$-100a_1A_{12}^4/A_{11}^2$
②	$20A_{11}^0/A_{11}^2$	⑱	$-100a_1A_{11}^4/A_{11}^2$
③	A_{12}^2/A_{11}^2	⑲	$-50a_1A_{22}^4/A_{22}^2$
④	A_{21}^2/A_{22}^2	⑳	$-50a_1A_{21}^4/A_{22}^2$
⑤	$10A_{21}^1/A_{22}^2$	㉑	$-500a_1A_{22}^3/A_{22}^2$
⑥	$10I_\alpha\omega_\alpha{}^2/A_{22}^2$	㉒	$\dfrac{-0.5a_1\left[A_{11}^3h(0) + A_{12}^3\theta(0)\right]S.F.}{A_{11}^2}$
⑦	$\dfrac{-10\left[2\pi\rho b^4\left(a + \frac{1}{2}\right)\right]}{A_{22}^2}$	㉓	$2\beta_1$
⑧	0.2	㉔	$\dfrac{-0.25a_2\left[A_{11}^3h(0) + A_{12}^3\theta(0)\right]S.F.}{A_{11}^2}$
⑨	0.2	㉕	$0.125a_2/a_1$
⑩	$0.0005h(0) \times S.F.$	㉖	$2\beta_2$
⑪	$10A_{11}^1/A_{11}^2$	㉗	$\dfrac{-0.25a_1\left[A_{21}^3h(0) + A_{22}^3\theta(0)\right]S.F.}{A_{22}^2}$
⑫	$10A_{12}^0/A_{11}^2$	㉘	$2\beta_1$
⑬	$10A_{12}^1/A_{11}^2$	㉙	$\dfrac{-0.125a_2\left[A_{21}^3h(0) + A_{22}^3\theta(0)\right]S.F.}{A_{22}^2}$
⑭	$0.001\theta(0) \times S.F.$	㉚	$0.125a_2/a_1$
⑮	$10A_{22}^1/A_{22}^2$	㉛	$2\beta_2$
⑯	$-250a_1A_{12}^3/A_{11}^2$		

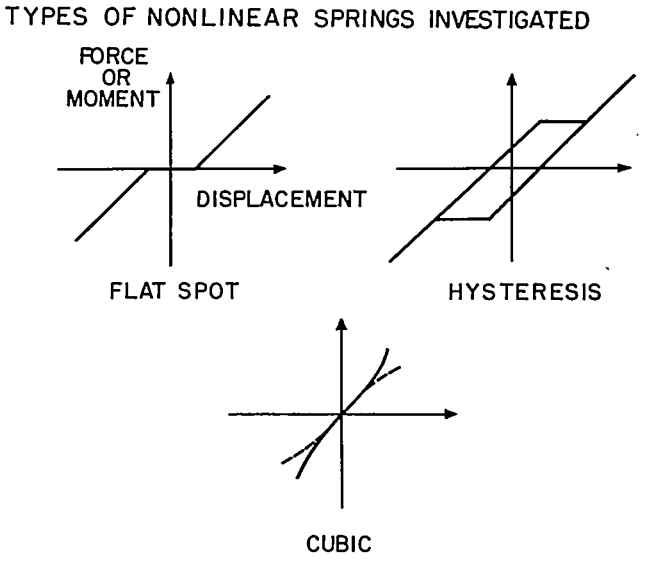

Figure 1

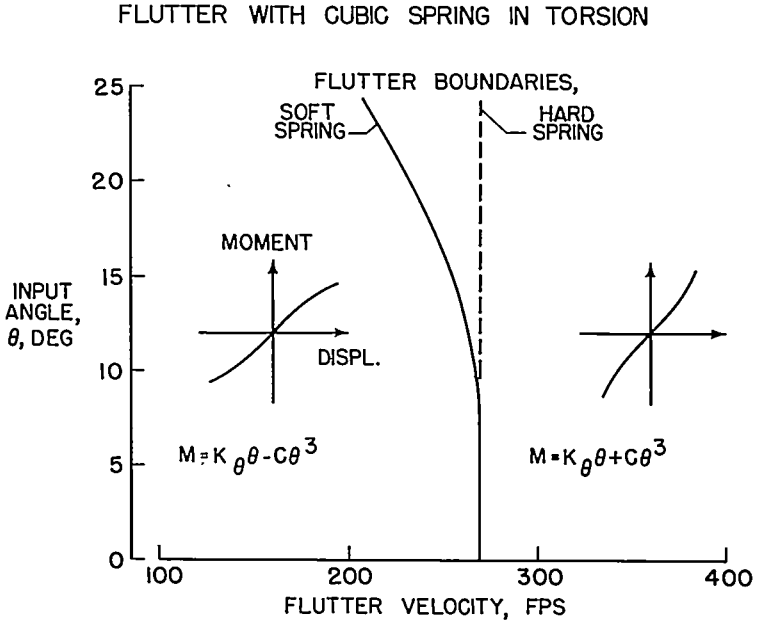

Figure 2

NONLINEAR FLUTTER MODEL

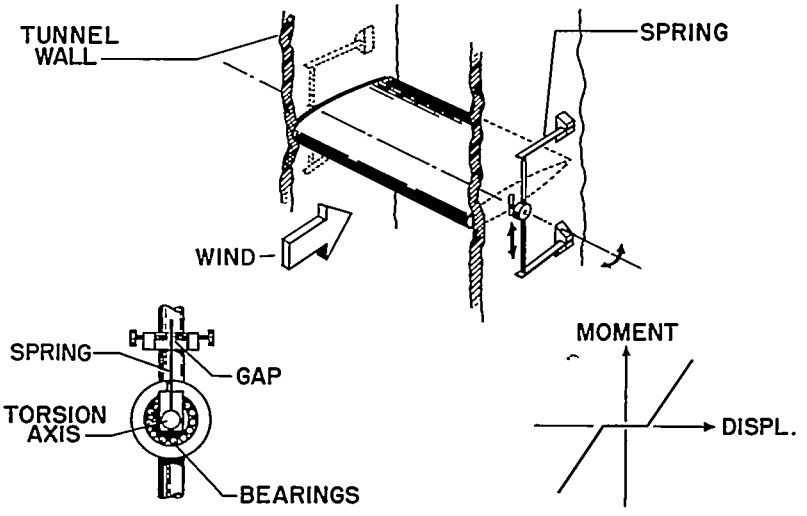

Figure 3

FLUTTER WITH FLAT SPOT IN TORSION

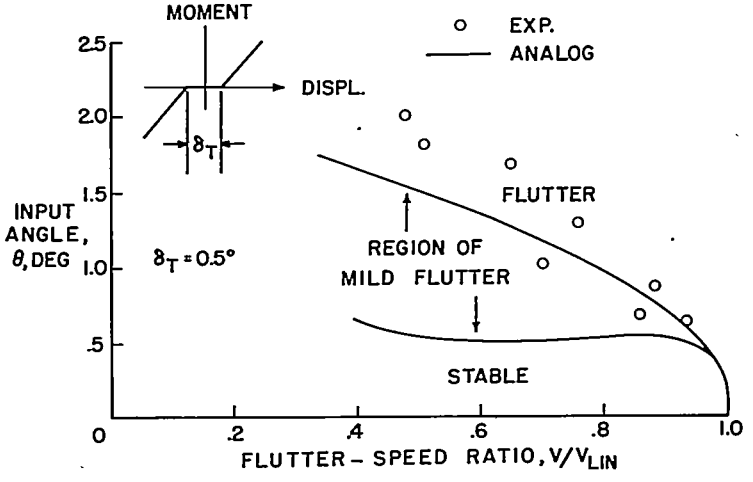

Figure 4

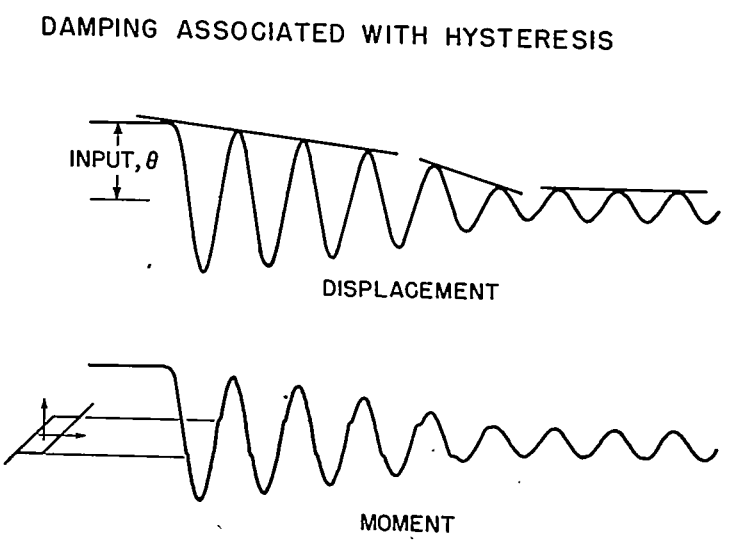

Figure 5

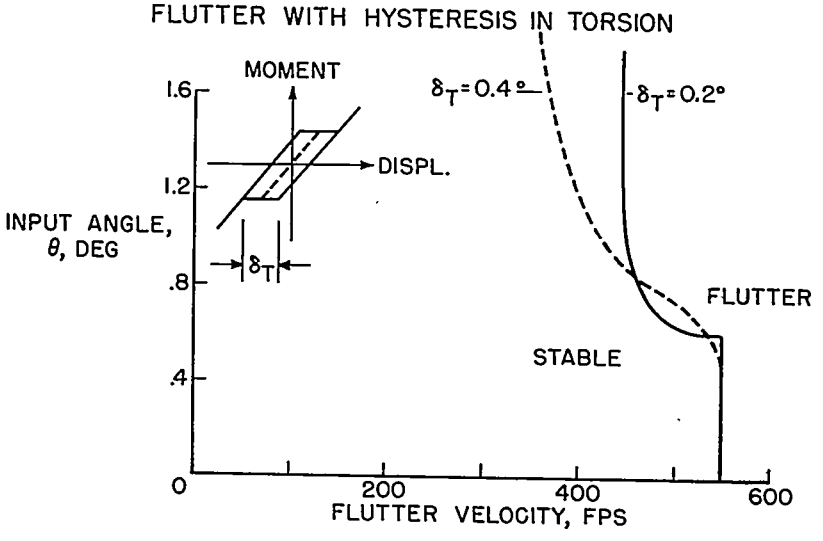

Figure 6

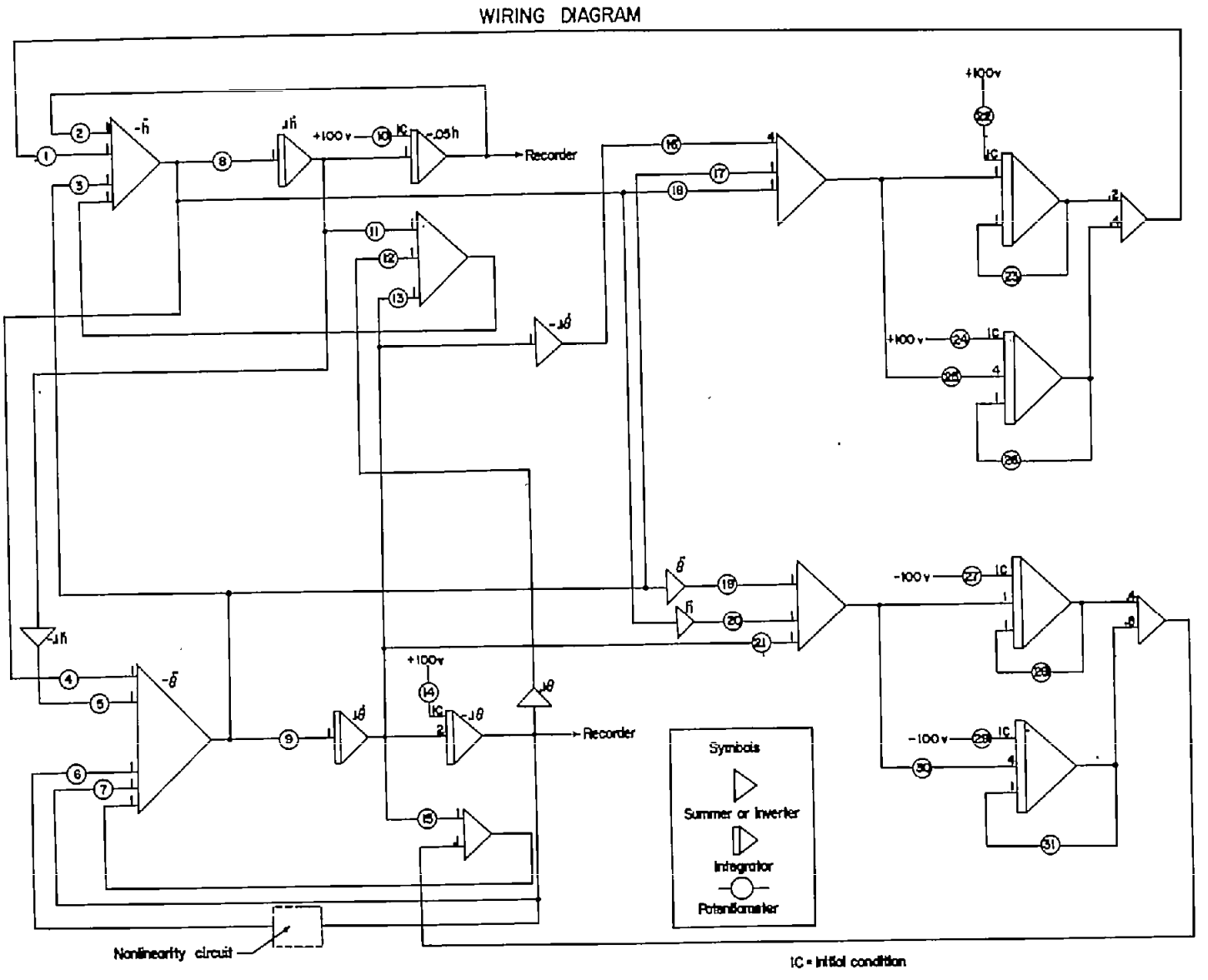
WIRING DIAGRAM
+100v
Recorder
Recorder
Symbols
Summer or Inverter
Integrator
Potentiometer
Nonlinearity circuit
IC = initial condition

Figure 7